

ORIGINAL RESEARCH ARTICLES

DESIGN, SYNTHESIS AND MOLECULAR MECHANISM OF FEW NEURAMINIDASE INHIBITORS IN TREATMENT OF H1N1 BY NMR TECHNIQUES

Jadhav P.^a, Borkar M.^a, Malbari K.^a, Joshi M.^b and Kanyalkar M.^{a*}

(Received 24 September 2018) (Accepted 17 January 2019)

ABSTRACT

Considering the issue of resistance to anti-influenza drugs, there is a need for discovery of new antiviral drugs. In view of this, flavones and their synthetic precursors i.e. chalcones were designed as inhibitors of influenza virus - H1N1 neuraminidase enzyme using structure-based drug design. Based on the best docking scores, some chalcone and flavone derivatives were synthesized and characterized by IR and proton NMR. Few of them were selected for ³¹P NMR studies, in order to probe the molecular mechanism of their antiviral action. Reasonably good correlation between docking scores and ³¹P NMR results were observed. As antiviral drugs are known to show membrane stabilizing effect on host cell, ³¹P NMR data for methoxy chalcone showed stabilization effect on model membrane pointing towards good antiviral activity which remained unaffected even after its cyclization to flavone. These derivatives can be explored further to provide a future therapeutic option for the treatment and prophylaxis of H1N1 viral infections.

Keywords: Anti-influenza activity; chalcone; flavone; ³¹P NMR; molecular mechanism

INTRODUCTION

Influenza is an acute viral infection caused by an influenza virus¹. The viral envelope consists of a lipid bilayer that contains three of the viral transmembrane proteins: haemagglutinin (HA), neuraminidase (NA), and matrix-2 (M2). The virus initially binds to sialic acid (SA)-linked host cell-surface receptors via the HA glycoprotein. The entry into the cell by endocytosis is then followed by the viral and endosomal membranes fusion under low pH conditions that further opens up M2 ion channel. NA mediates release of the virus particle from the host cell by cleaving the glycosidic linkage between SA-linked host cell-surface receptor and HA. Thus, NA is responsible for facilitating the spread of infection to other host cells^{2,3}. There are three types of influenza viruses – A, B and C. Influenza A virus infect many species including birds and mammals while influenza subtype B and C virus infect essentially humans⁴. The distinct antigenic properties of different HA and NA molecules are used to classify influenza type A viruses into subtypes: sixteen for HA (H1-H16) and nine for NA (N1-N9)⁵.

Currently, there are two classes of anti-influenza drugs available for the treatment of influenza viruses, the M2 proton channel inhibitors (adamantanes) and the NA inhibitors. First-generation anti-influenza drugs, the adamantanes, show limited scope because of lack of activity attributed to resistance and unwanted side effects⁶. One of the main advantages of the second-generation anti-influenza agents, i.e. NA inhibitors, is that they are active against both influenza A as well as influenza B with improved safety profile, and lower potential for inducing resistance⁷. Fortunately, viruses that develop resistance to the adamantanes remain susceptible to NA inhibitors. These NA inhibitors viz. oseltamivir and zanamivir, which are the transition state derivatives of endogenous ligand sialic acid, are the only commercially available lines of treatment for influenza^{8,9}. But a report says that N1 subtype of influenza virus has become resistant to oseltamivir due to mutations: (1) His274Tyr; (2) Asn294Ser; and (3) Tyr252His¹⁰. Also, the mutation Gln136Lys increases the mobility of Asp151 and Arg156 groups by breaking their bonding network leading to resistance to Zanamivir¹¹. Hence, there is an utmost need of the third-generation anti-influenza which can address the issue of resistance.

^a Prin K. M. Kundnani College of Pharmacy, Cuffe Parade, Mumbai - 400 005, Maharashtra, India

^b National Facility for High Field NMR, Tata Institute of Fundamental Research, Homi Bhabha Road, Mumbai-400 005, Maharashtra, India

*For Correspondence: Email: meenatul@gmail.com

<https://doi.org/10.53879/id.56.02.11584>

Many scaffolds were developed based on similar structural features of endogenous ligand¹². All studies so far have been focused on the attachment of new chemical group with a proper shape, size and electronic charge for fitting into the active site¹³. Phytoconstituents such as chalcones (1,3-diphenyl-2-propene-1-ones) and flavones(2-phenyl-4h-chromen-4-one) are known to exert anticarcinogenic, antimicrobial, antiprotozoan, antipsoriasis, antineurodegenerative, antidiabetic, and antiviral properties^{14,15}. Keeping in mind the structural resemblance of oseltamivir with sialic acid, we have focused on chalcones and flavones that are structurally diverse molecules from oseltamivir and sialic acid. Chalcones and flavones structurally belong to largest polyphenolic class of plant secondary metabolites. They are considered as precursors of flavonoids and isoflavonoids which are abundant in edible plants with therapeutic value and are known to inhibit enzyme glycosidase. Neuraminidase is a class of glycosidase and is reported that chalcones as well as flavones acts by inhibiting it. They act as receptors where many diverse compounds can bind¹⁶.

In this paper, we have considered chalcones and their cyclic counterparts, flavones, as prototype and further developed them using molecular modelling approach followed by its synthesis (Table I). We have carried out cytotoxicity studies of the synthesized derivatives. We have then focused on studying interactions of selected derivatives of the above scaffolds with lipid biomembrane/bilayers. Interaction of several classes of drug with constituents of biomembrane, especially phospholipids, play a key role in their pharmacological action. Basic understanding of interaction of drug molecule with lipid bilayer is crucial to get an insight of their mechanism. Some drugs interact with phospholipids of lipid bilayer and induce modification in physicochemical state of the bilayer⁸. For example, antifungal drugs interact with lipid bilayer of fungal cells where they produce fusiogenic effect. On other hand, antiviral drug stabilize the host bilayer to produce membrane stabilizing effect^{17,18}. Thus, we have probed the molecular interactions of our synthesized derivatives with phospholipid bilayers, using multidimensional and multinuclear NMR techniques that gauge the effect of the derivatives on the polymorphism and membrane stabilizing effect on bilayers. In this study, L- α - dipalmitoylphosphatidylcholine (DPPC) is used as model membrane. The results of interaction studies, used to confirm the membrane stabilizing effect produced by our derivatives, is one of the characteristics of antiviral drugs.

MATERIALS AND METHODS

Materials

2, 4-Dihydroxy acetophenone and various substituted benzaldehydes were purchased from S. D. Fine-Chem Ltd., India. L- α -Diapalmitoylphosphatidyl choline (DPPC) was purchased from Sigma Chemicals Co., U.S.A. All other solvents used for synthesis were of LR grade.

METHODS

Computational studies

Computational studies were carried out with the modelling package Discovery Studio (DS) 3.1 (Accelrys Inc., USA)¹⁹ running on a Windows 7 Platform. Docking studies were carried out with GOLD v 5.0.1 (CCDC, UK)²⁰ running on a CentOS 6 platform Linux Workstation.

Preparation of enzyme and ligand for docking

The enzyme H1N1-NA in complex with oseltamivir (OMV) was taken (PDB code no. 3TI6)²¹, solved by X-ray crystallography, representing pandemic enzyme. Monomeric unit of the dimeric enzyme was used for docking studies. After removal of crystallographic water molecule, hydrogen atoms were added, atom types and partial charges were assigned based on the CHARMM forcefield. Formal charges for the acidic and basic amino acids were set according to the physiological condition at pH 7.4. Acetyl (ACE) and N-methyl-amino groups were used to cap N- and C-termini, respectively. The system was refined using the CHARMM forcefield to a gradient of 0.1 kcal/mol/Å. The oseltamivir, zanamivir and designed ligand structures were energy minimized using the "Smart Minimizer" method in energy minimization with the CHARMM forcefield to a gradient of 0.01 kcal/mol/Å. The docked poses were scored using GoldScore. The non-bonded interaction energy calculations contributed by van der-Waals (vdW) and Electrostatic (Ele) energies were done by using "Simulation" module of DS 3.1.

Docking Protocol

The parameters in GOLD were, kept similar as in our previously published work¹⁴. The receptor active site was shaped by residues in a 10 Å vicinity of ligand OMV. At the start of a docking run, all the variables were randomized in order to validate the protocol. Docking of OMV was carried out for 20 genetic algorithm (GA) runs, which was found sufficient to reproduce the binding pose of OMV in PDB 3TI6. The validated protocol was used to dock the designed chalcone and flavone derivatives in H1N1-NA to determine their preferred binding orientations.

Synthesis of derivatives of chalcones

We have selected and synthesized various substituted chalcone and flavone derivatives with different substitutions such as chloro, methoxy, hydroxy and nitro at benzylidene moiety while keeping the 2, 4-dihydroxyphenyl group in chalcone and 7-hydroxy-4h-chromen-4-one group in flavone constant in structure (Table I). Completion of the reactions was monitored by TLC using n-hexane: ethyl acetate (3:2) solvent system. The structure and purity of the starting materials and final compounds were confirmed by physical constants, TLC and spectral techniques like IR and NMR spectroscopy. The synthesized and purified analogues were characterized by spectral techniques: IR and ¹H NMR spectroscopy. The IR spectra of the synthesized analogues represented expected absorption bands for the functional groups. The analogues exhibited predictable delta values for all aliphatic and aromatic protons in ¹H NMR spectra. Thus, the correctness of anticipated structures of the synthesized analogues was confirmed by the spectroscopy^{22,23}.

Synthesis of 2', 4'-dihydroxychalcone

The series of derivatives of chalcone were synthesized by Claisen-Schmidt condensation. Equimolar quantities (1 mol) of substituted acetophenone and substituted benzaldehyde were dissolved in absolute ethanol. Sodium hydroxide solution (20%, 10 mL) was added to this solution at 10°C and the resulting mixture was stirred at room temperature (temperature increased gradually). The precipitate obtained was neutralised with conc. HCl and then filtered and recrystallized using ethanol. Some of the derivatives of this series are reported to be synthesized elsewhere by method other than mentioned above²².

1-(2', 4'-dihydroxyphenyl)-3-phenylprop-2-en-1-one (1a). Yellow solid, m.p. 157° C. IR (KBr) ν_{\max} 3384-3494 (OH), 1632 (C=O), 1600 (C=C); ¹H-NMR (DMSO-d₆, 500 MHz) δ ppm 13.37 (bs, 1H, 2'-OH), 12.59 (bs, 1H, 4'-OH), 8.21-8.19 (d, 3H, H-2, H-5', H-6'), 8.00-7.97 (t, 1H, H-5''), 7.75-7.73 (t, 2H, H-3'', H-4''), 7.46 (s, 1H, H-3'), 6.42-6.33 (d, 3H, H-3, H-2'', H-6'').

1-(2', 4'-dihydroxyphenyl)-3-(2''-hydroxyphenyl)-prop-2-en-1-one (1b). Yellow solid, m.p. 135° C. IR (KBr) ν_{\max} 3316 (OH), 1672 (C=O), 1606 (C=C); ¹H-NMR (DMSO-d₆, 500 MHz) δ ppm 12.63 (bs, 1H, 2'-OH), 10.63 (bs, 2H, 4'-OH, 2''-OH), 7.79-7.77 (d, 3H, H-2, H-5', H-6''), 6.96-6.94 (t, 2H, H-4'', H-5''), 6.40-6.39 (d, 2H, H-3, H-6''), 6.27 (s, 1H, H-3').

1-(2', 4'-dihydroxyphenyl)-3-(3''-hydroxyphenyl)-prop-2-en-1-one (1c). Yellow solid, m.p. 140° C. IR (KBr) ν_{\max} 3203 (OH), 1672 (C=O), 1605 (C=C); ¹H-NMR

(DMSO-d₆, 500 MHz) δ ppm 12.60 (bs, 1H, 2'-OH), 9.44 (bs, 2H, 4'-OH, 3''-OH), 9.86 (s, 1H, H-2''), 7.81-7.77 (d, 2H, H-5', H-6'), 7.02-7.01 (d, 2H, H-2, H-4''), 6.45-6.44 (t, 1H, H-5''), 6.337-6.334 (d, 2H, H-3, H-6''), 6.33 (s, 1H, H-3').

1-(2', 4'-dihydroxyphenyl)-3-(4''-hydroxyphenyl)-prop-2-en-1-one (1d). Yellow solid, m.p. 158° C. IR (KBr) ν_{\max} 3370 (OH), 1672 (C=O), 1606 (C=C); ¹H-NMR (DMSO-d₆, 500 MHz) δ ppm 12.74 (bs, 1H, 2'-OH), 10.92 (bs, 1H, 4'-OH), 9.787 (bs, 1H, 4''-OH), 7.76-7.74 (d, 3H, H-2, H-5', H-6''), 7.00-6.98 (d, 2H, H-3'', H-5''), 6.44-6.42 (d, 3H, H-3, H-2'', H-6''), 6.33 (s, 1H, H-3').

1-(2', 4'-dihydroxyphenyl)-3-(3'', 4''-dihydroxyphenyl)-prop-2-en-1-one (1e). Yellow solid, m.p. 180° C. IR (KBr) ν_{\max} 3385 (OH), 1673 (C=O), 1605 (C=C); ¹H-NMR (DMSO-d₆, 500 MHz) δ ppm 12.59 (bs, 2H, 2'-OH, 4'-OH), 9.69 (bs, 2H, 3''-OH, 4''-OH), 7.75-7.73 (d, 2H, H-2, H-5'), 7.28-7.24 (d, 1H, H-6''), 7.11 (s, 1H, H-2''), 6.98-6.97 (d, 1H, H-6''), 6.84-6.82 (d, 1H, H-3), 6.43-6.42 (d, 1H, H-5''), 6.33 (s, 1H, H-3').

1-(2', 4'-dihydroxyphenyl)-3-(2''-methoxyphenyl)-prop-2-en-1-one (1f). Yellow solid, m.p. 110° C. IR (KBr) ν_{\max} 3388 (OH), 1625 (C=O), 1500 (C=C); ¹H-NMR (DMSO-d₆, 500 MHz) δ ppm 12.60 (bs, 1H, 2'-OH), 10.63 (bs, 1H, 4'-OH), 7.95-7.93 (d, 2H, H-2, H-3), 7.76-7.75 (d, 2H, H-5', H-6''), 7.57-7.56 (d, 1H, H-3''), 7.38-7.33 (d, 1H, H-5'), 6.39-6.37 (d, 1H, H-6'), 6.25 (s, 1H, H-3'), 4.48 (s, 3H, 2''-OCH₃).

1-(2', 4'-dihydroxyphenyl)-3-(3'', 4''-dimethoxyphenyl)-prop-2-en-1-one (1g). Yellow solid, m.p. 190° C. IR (KBr) ν_{\max} 3207 (OH), 1632 (C=O), 1596 (C=C); ¹H-NMR (DMSO-d₆, 500 MHz) δ ppm 13.57 (bs, 1H, 2'-OH), 10.82 (bs, 1H, 4'-OH), 8.22 (s, 1H, H-2''), 7.86-7.84 (d, 1H, H-5'), 7.56 (s, 1H, H-3'), 7.40-7.39 (d, 1H, H-5''), 7.03-7.02 (d, 1H, H-6''), 6.466-6.463 (d, 1H, H-6''), 6.45-6.32 (d, 2H, H-2, H-3), 3.87 (s, 3H, 3''-OCH₃), 3.82 (s, 3H, 4''-OCH₃).

1-(2', 4'-dihydroxyphenyl)-3-(3'', 4'', 5''-trimethoxyphenyl)-prop-2-en-1-one (1h). Yellow solid, m.p. 195° C. IR (KBr) ν_{\max} 3336 (OH), 1630 (C=O), 1592 (C=C); ¹H-NMR (DMSO-d₆, 500 MHz) δ ppm 13.55 (bs, 1H, 2'-OH), 12.76 (bs, 1H, 4'-OH), 8.12-8.10 (d, 2H, H-2, H-3), 7.93 (s, 1H, H-2''), 7.81-7.80 (d, 2H, H-5', H-6'), 7.35 (s, 1H, H-6''), 6.50 (s, 1H, H-3'), 3.95 (s, 3H, 3''-OCH₃), 3.92 (s, 3H, 5''-OCH₃), 3.83 (s, 3H, 4''-OCH₃).

1-(2', 4'-dihydroxyphenyl)-3-(4''-chlorophenyl)-prop-2-en-1-one (1i). Yellow solid, m.p. 199° C. IR (KBr) ν_{\max} 3308 (OH), 1632 (C=O), 1606 (C=C); ¹H-NMR

(DMSO- d_6 , 500 MHz) δ ppm 12.59 (bs, 1H, 2'-OH), 10.95 (bs, 1H, 4'-OH), 7.95-7.93 (d, 2H, H-5', H-6'), 7.75-7.73 (d, 2H, H-3'', H-5''), 7.58-7.56 (d, 2H, H-2'', H-6''), 7.47-7.37 (d, 2H, H-2, H-3), 6.33 (s, 1H, H-3').

Synthesis of flavone

Chalcone, obtained as mentioned above, was suspended in DMSO (10 mL) and a crystal of iodine was added to it. The reaction mixture was refluxed for 1h and then poured on crushed ice. The solid obtained was filtered off, washed with 20% sodium thiosulphate and recrystallized using ethanol. Some of the derivatives of this series are reported to be synthesized elsewhere by method other than mentioned above²³.

7-Hydroxy-2-phenyl-4H-chromen-4-one (2a).

White solid, yield (84%), m.p. 247° C. IR (KBr) ν_{\max} 3595 (OH), 1624 (C=O), 2699 (C=C alkene and aromatic), 1508 (C-O-C); ¹H-NMR (DMSO- d_6 , 500 MHz) δ ppm 10.83 (bs, 1H, 7-OH), 8.092-8.078 (d, 3H, H-5, H-2', H-6'), 7.92-7.90 (d, 1H, H-6), 7.60-7.59 (t, 2H, H-3', H-5'), 7.032 (s, 1H, H-8), 6.96-6.95 (t, 1H, H-4'), 6.92 (s, 1H, H-3).

7-Hydroxy-2-(4'-methoxyphenyl)-4H-chromen-4-one (2b). White solid, m.p. 210° C. IR (KBr) ν_{\max} 3420 (OH), 1631 (C=O), 1684 (C=C alkene and aromatic), 2596 (C-O-C); ¹H-NMR (DMSO- d_6 , 500 MHz) δ ppm 12.64 (bs, 1H, 7-OH), 7.97-7.95 (d, 1H, H-5), 7.76 (s, 1H, H-8), 7.59-7.57 (d, 1H, H-6), 7.40-7.34 (d, 2H, H-2', H-6'), 6.41-6.39 (d, 2H, H-3', H-5'), 6.27 (s, 1H, H-3).

7-Hydroxy-2-(3'-chlorophenyl)-4H-chromen-4-one (2c). White solid, m.p. 225° C. IR (KBr) ν_{\max} 3076 (OH), 1695 (C=O), 1606 (C=C alkene and aromatic), 1695 (C-O-C), 720 (Cl); ¹H-NMR (DMSO- d_6 , 500 MHz) δ ppm 13.30 (bs, 1H, 7-OH), 8.074 (s, 1H, H-2'), 7.92 (s, 1H, H-8), 7.73-7.71 (d, 2H, H-5, H-4'), 7.58-7.55 (t, 1H, H-5'), 7.41-7.38 (d, 1H, H-6), 7.06 (s, 1H, H-3), 6.97-6.95 (d, 1H, H-6').

7-Hydroxy-2-(4'-chlorophenyl)-4H-chromen-4-one (2d). White solid, m.p. 198° C. IR (KBr) ν_{\max} 3445 (OH), 1710 (C=O), 1605 (C=C), 700 (Cl); ¹H-NMR (DMSO- d_6 , 500 MHz) δ ppm 12.64 (bs, 1H, 7-OH), 7.97-7.95 (d, 2H, H-3', H-5'), 7.76 (s, 1H, H-8), 7.59-7.57 (d, 1H, H-5), 7.40-7.34 (d, 2H, H-2', H-6'), 6.41-6.39 (d, 1H, H-6), 6.27 (s, 1H, H-3).

7-Hydroxy-2-(4'-nitrophenyl)-4H-chromen-4-one (2e). Yellow solid, m.p. 230° C. IR (KBr) ν_{\max} 3412 (OH), 1614 (C=O), 1567 (C=C), 1757 (C-O-C), 1471 (NO₂); ¹H-NMR (DMSO- d_6 , 500 MHz) δ ppm 13.37 (bs, 1H, 7-OH), 8.19-8.17 (d, 2H, H-3', H-5'), 7.86-7.89 (d, 1H, H-5), 7.71-

7.68 (d, 2H, H-2', H-6'), 7.32 (s, 1H, H-8), 7.28-7.24 (d, 1H, H-6), 6.30 (s, 1H, H-3).

Sample preparation for drug-lipid interaction studies using ³¹P NMR

Multilamellar vesicles (MLVs) were prepared by the standard procedure¹⁴ wherein the desired quantity of DPPC and chalcone derivative was dissolved in chloroform. The solvent was then evaporated with a stream of nitrogen so as to deposit a lipid film on the walls of the container. The last traces of the solvent were removed with freeze drying for a period of 1 h. The lipid film was hydrated with the required amount of D₂O; this was then incubated in a water bath at 50°C with repeated vortexing. The lipid concentrations were maintained at 100 mM for the NMR and 50 mM for the DSC experiments. Unilamellar vesicles (ULVs) were prepared by sonicating the above dispersions with a Branson sonicator (Model 450) at 50% duty cycles till the solution was optically clear.

NMR experiments

NMR experiments were recorded on a BRUKER AVANCE 500 MHz and 700 MHz NMR spectrometer. Resonance assignments were carried out using 1D proton NMR spectra which were recorded using standard pulse program. ³¹P experiments were carried out with a relaxation delay of 1 s and broadband proton decoupling²⁴⁻²⁶. The NMR data was processed with Topspin 2.1 software.

RESULTS

Docking

The initial validation studies with the docking protocol could satisfactorily reproduce (RMSD 0.52 Å) the binding conformation of the OMV in 3TI6. All the interactions are consistent with original crystal structure of OMV in PDB code 3TI6. There are four well-conserved binding sites in H1N1-NA active site, which was discussed in our previous work¹⁴, with 11 functional residues which participate in the catalytic reaction¹. These are the positively charged site-1 (Arg118, Arg292 and Arg371), the negatively charged site-2 (Glu119, Glu227 and Asp151), site-3 (Ile222 and Tyr178), and site-4 (Glu276 and Glu277). Moreover, presence of the 150-loop (residues 147-152), that exists in two stable conformations (closed and open), forms one part of the enzyme active site. It was reported that initially oseltamivir binds to "open" form of NA. Subsequently, it results into "closed" form by undergoing a conformational change⁵. Interestingly, the crystal structure of NA from the 2009 pandemic H1N1 influenza strain indicates that it lacks the 150 loop in its active site (similar to closed

conformation)²⁷. This indicates importance of open and closed conformations of 150-loop in the design of newer NA inhibitors. Further, literature survey on molecular modelling studies of OMV indicates that the neuraminidase molecule undergoes rearrangement to create an additional binding pocket to accommodate the hydrophobic side chain of oseltamivir in the active site^{28,29}. The binding pocket is formed when the amino acid Glu276 rotates due to ionic interaction with Arg224 and binds with it. But, the ionic interaction between Glu276 and Arg224 is prevented owing to the mutations Arg292Lys, Asn294Ser, and His274Tyr, due to which the rotation of Glu276 is inhibited.

The hydrogen bonding interactions and molecular surface model of representative chalcone and flavone derivatives with NA active site in 3TI6 are depicted in Fig. 1. The hydrogen bonds formed between the substrate/inhibitors and the enzyme are summarized in Table II. All the chalcone derivatives showed better interactions with Agr118, Arg292 and Arg371 at site-1 and as that of OMV, but adapt completely different interactions at other sites. In most of the designed chalcone derivatives, aromatic ring containing dihydroxy group interacts with site-1 and substituted aromatic ring interacted with site-3 and site-4. It was observed that in the chloro substituent chalcone (**1i**) they were inclined outside the cavity, while hydroxyl (**1b**) and methoxy (**1f**) chalcones interacted in site-3 and site-4. All hydroxyl derivatives showed better fit in site-4 with Glu277.

Unsubstituted flavone (**1a**) and chloro flavone (**2c** and **2d**) interacted with site-2. Methoxy flavone (**2b**) interacted with site-1 and site-4 like OMV. In nitro flavone (**2e**), nitro group interacted with site-4.

Drug-lipid interaction

The study of interaction between drug and lipid bilayer gives a lot of information on membrane fluidity, stability and polymorphism of the bilayer. Studies have shown that stabilization of the membrane by antiviral drug can play an important role in inhibiting membrane fusion and also antiviral activity¹⁸. With this in view we have carried out drug-lipid bilayer interaction studies using multinuclear NMR technique. We have used DPPC as model membrane for ³¹P interaction studies with respect to docking results observed. We have selected **1d** (2', 4'-dihydroxy-4''-hydroxy chalcone), **1g** (2', 4'-dihydroxy-3'', 4''-dimethoxy chalcone), **1i** (2', 4'-dihydroxy-4''-chloro chalcone) and **2b** (7-hydroxy-4'-methoxy flavone) to study the drug-lipid interactions.

³¹P NMR

In order to understand the intermolecular interaction between derivatives and the lipid membrane, ³¹P NMR experiments had been carried out for our synthesized chalcone and flavone derivatives in presence of the lipid bilayers of DPPC that serves as model membrane. ³¹P NMR spectroscopy is widely used for studies of phospholipid bilayers and biological membranes in native conditions. The analysis of ³¹P NMR spectra of lipids provide information about lipid bilayer packing, phase transitions, lipid head group orientation/dynamics, and elastic properties of pure lipid bilayer in native state and after binding with proteins and other biomolecules³⁰. Lipid bilayers give a characteristic broad spectrum with a high field peak and low field ³¹P line shoulder. The ³¹P NMR resonance line shape was determined by the chemical shift anisotropy (CSA) (measured from the low σ_{\parallel} and high σ_{\perp} field shoulders of the spectrum, $\Delta\sigma = \sigma_{\perp} - \sigma_{\parallel}$) of the phosphate group coupled with the molecular motions near the bilayer head groups³¹.

The change in ³¹P NMR line shape of lipid bilayers incorporated with increasing concentrations of selected derivatives is shown in Fig. 2. In each case the lower most graphs represent the ³¹P NMR line shape for lipid bilayers alone (Fig. 2 DPPC). In a randomly oriented sample such as DPPC dispersions in the gel phase, the overall rotational rate is slow. One observes a sharp signal at -20 ppm from lipid molecules with their long axis oriented perpendicular to the direction of the magnetic field (σ_{\perp}), while for the parallel alignment of the lipid molecules (σ_{\parallel}) a broad shoulder appears at 25 ppm. A relatively small but sharp peak is observed at 0 ppm due to the formation of a small amount of unilamellar vesicles with a small size that permits fast internal and tumbling motions. It may be noted here that these molecules do not alter the characteristic line shapes exhibiting bilayer features of the MLV's of lipid at all concentrations.

In the case of **1d** (2', 4'-dihydroxy-4'-hydroxy chalcone), with increasing concentration, parallel peak became broad and shifted towards the perpendicular peak. The perpendicular peak at 1:10, 1:5 and 1:2 became broad except for 1:1 which remained unaffected. This indicated that there was slight perturbation of the lipid bilayer structure as the drug concentration goes on increasing (Fig. 2. **1d**). In case of **1g** (2', 4'-dihydroxy-3'', 4''-dimethoxy chalcone), ³¹P line shape was not affected and remained very similar to DPPC. Line shape features of bilayer structure remained unchanged, similar to DPPC. It was observed that the perpendicular peak slightly broadened as the concentration of drug increased.

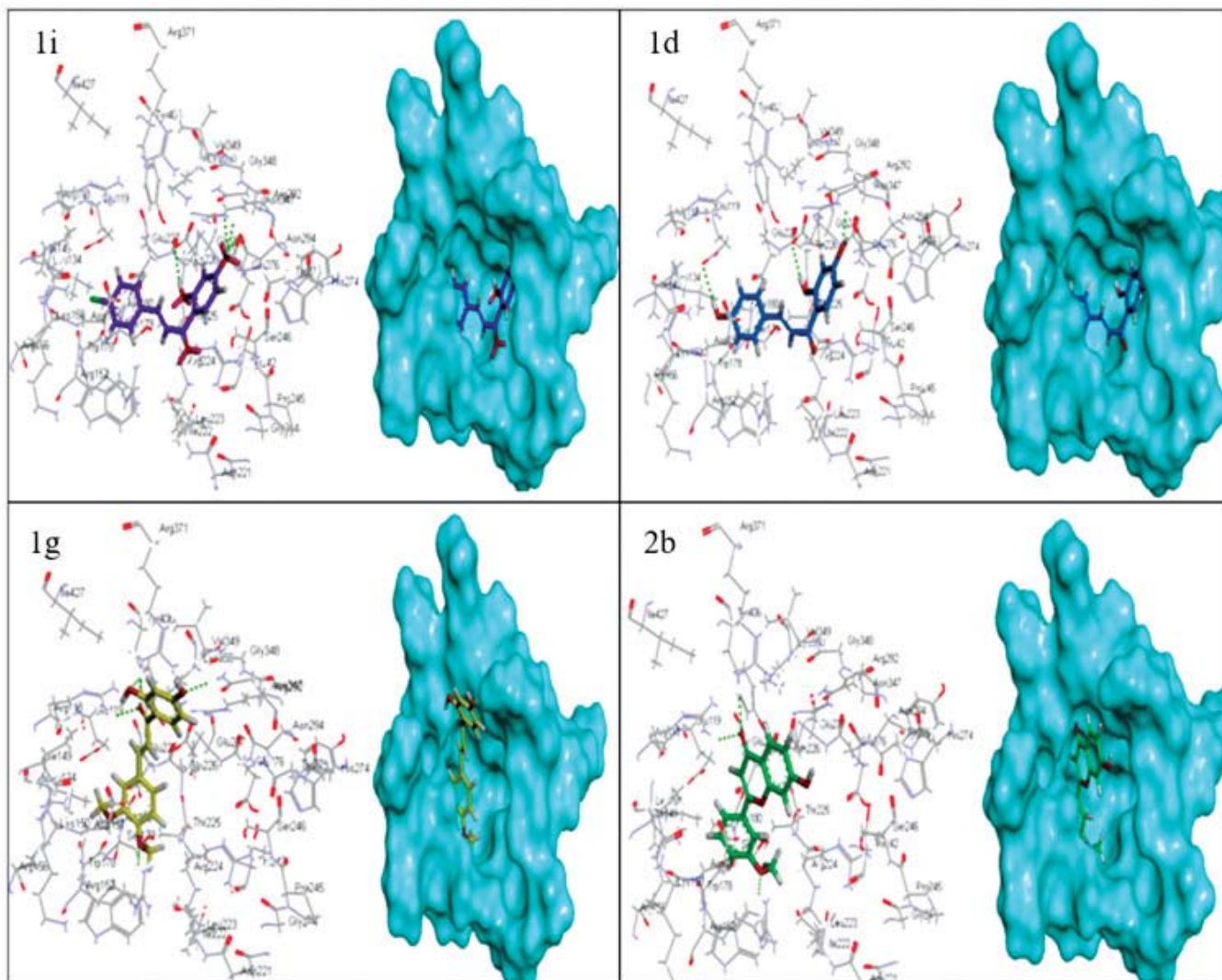


Fig. 1: Docked poses of 1d (2', 4'-dihydroxy-4''-hydroxychalcone), 1g (2', 4'-dihydroxy-3'', 4''-dimethoxychalcone), 1i (2', 4'-dihydroxy-4''-chloro chalcone) and 2b (7-hydroxy-4'-methoxyflavone)

Moreover, the bilayer features remained intact to a large extent keeping the vesicles highly rigid. This suggested that **1g** imparted very little perturbation to the bilayer (Fig. 2. **1g**) and produced membrane stabilizing effect. In case of **1i** (2', 4'-dihydroxy-4''-chloro chalcone), ^{31}P line shape changed as the concentration of the drug varied and was slightly different from that of DPPC. But the parallel peak did not completely vanish, indicating that there was membrane stabilizing effect. At the drug: lipid molar ratio of 1:10, the line shape features of bilayer structure remained unchanged and very similar to that of DPPC. When the concentration of the drug was the highest, the perpendicular peak remained at -20 ppm while the parallel peak shifted towards the perpendicular peak. At the drug: lipid molar ratio of 1:10 and 1:2, the perpendicular peak broadened. The effect of **1i** perturbed

the bilayer phase. Thus, it was observed that there was a perturbation of the lipid bilayer as the drug concentration varied (Fig. 2. **1i**). In case of **2b** (7-hydroxy-4'-methoxy flavone), the parallel peak remained unaffected while the perpendicular peak broadened as the drug concentration goes on increasing. The bilayer features remained intact to a large extent keeping the vesicles highly rigid. This suggested that **2b** also imparted very little perturbation to the bilayer (Fig. 2. **2b**).

DISCUSSION

The ^{31}P NMR studies along with molecular docking revealed that methoxy substituted chalcone and flavone showed membrane stabilizing effect on DPPC bilayer and good receptor interaction with pandemic NA. As antiviral drugs are known to show membrane stabilizing

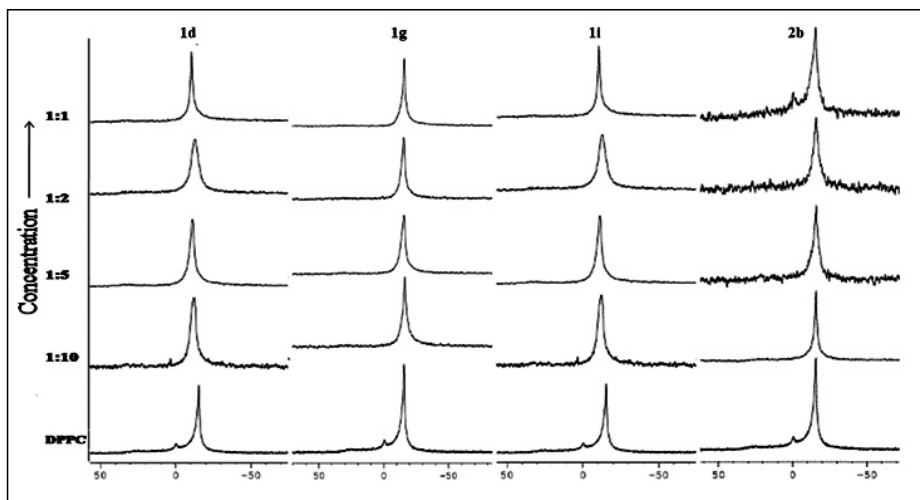


Fig. 2: 500 MHz concentration dependent ^{31}P NMR spectra of DPPC (100 mmol/L) multilamellar vesicles incorporated with 1d (2', 4'-dihydroxy-4''-hydroxy chalcone), 1g (2', 4'-dihydroxy-3'', 4''-dimethoxy chalcone), 1i (2', 4'-dihydroxy-4''-chloro chalcone) and 2b (7-hydroxy-4'-methoxy flavone). The additive: lipid molar ratios are (A) 0:10, (B) 1:5, (C) 1:2, and (D) 1:1. All experiments are at 323 K

effect on host cell, it further justifies the point that methoxy chalcone showed good antiviral activity which remained unaffected even after its cyclization to flavone derivatives. From the above results, we can conclude that chalcone and flavone which are not "me too" type of scaffolds as that of oseltamivir and zanamivir show antiviral properties evident from ^{31}P NMR studies and computational studies.

ACKNOWLEDGEMENTS

M. A. Kanyalkar thanks Indian Council of Medical Research (ICMR), New Delhi for funding computational facilities at Prin. K. M. Kundnani College of Pharmacy through

Table I: Designed chalcone and flavone scaffolds

Scaffolds	Code	R ₁	R ₂	R ₃	R ₄
	1a	H	H	H	H
	1b	OH	H	H	H
	1c	H	OH	H	H
	1d	H	H	OH	H
	1e	H	OH	OH	H
	1f	OCH ₃	H	H	H
	1g	H	OCH ₃	OCH ₃	H
	1h	H	OCH ₃	OCH ₃	OCH ₃
	1i	H	H	Cl	H
	2a	H	H	H	H
	2b	H	H	OCH ₃	H
	2c	H	Cl	H	H
	2d	H	H	Cl	H
	2e	H	H	NO ₂	H

Table II: Atoms of 1d (2', 4'-dihydroxy-4''-hydroxy chalcone), 1g (2', 4'-dihydroxy-3'', 4''-dimethoxy chalcone), 1i (2', 4'-dihydroxy-4''-chloro chalcone), 2b (7-hydroxy-4'-methoxyflavone) and amino acid residues involved in Hydrogen bonding with 3TI6 protein. Last row indicates number of H-bonds formed

Amino acid residues	1d	1g	1i	2b
SITE1	-	-	-	-
ARG118	-	C=O... NH	-	OH...NH
ARG292	OH... NH	-	OH... NH	-
ARG371	-	OH...NH C=O... NH	-	-
SITE2				
GLU119	OH...O- C=O	-	-	-
ASP151	-	-	-	-
GLU227	-	-	-	-
SITE 3				
TRP178	-	-	-	-
ILE222	-	-	-	-
SITE 4				
GLU276	-	-	-	-
GLU277	OH...O- C=O	-	OH... O-C=O	-
ARG156	-	-	-	-
SER176	-	-	-	OCH ₃ ... NH
ARG156	-	OCH ₃ ... NH	-	-
ASP151	-	-	-	-
ASN347	-	OH...NH	-	-
H Bonds	5	5	3	2

Adhoc research scheme (58/36/2013-BMS). K. D. Malbari thanks ICMR, New Delhi for Senior Research Fellowship (58/36/2013-BMS). Authors greatly acknowledge the NMR facility provided by TIFR, Mumbai.

REFERENCES

- Colman P. M.; Varghese J. N.; Laver W. G.: Structure of the Catalytic and Antigenic Sites in Influenza Virus Neuraminidase, *Nature*, 1983, 303 (5912), 41–44.
- Liu C.; Eichelberger M. C.; Compans R. W.; Air G. M.: Influenza Type A Virus Neuraminidase Does Not Play a Role in Viral Entry, Replication, Assembly, or Budding, *J. Virol.*, 1995, 1099–1106.
- Palese P.; Tobita K.; Ueda M.; Compans R. W.: Characterization of Temperature Sensitive Influenza Virus Mutants Defective in Neuraminidase, *Virol.*, 1974, 61 (2), 397–410.
- Hayden F. G.; de Jong M. D.: Emerging Influenza Antiviral Resistance Threats, *J. Infect. Dis.*, 2011, 203 (1), 6–10.
- Chintakrindi A.; Kanyalkar M.; D'Souza C.: Rational Development of Neuraminidase Inhibitor as Novel Anti-Flu Drug, *Mini-Rev. Med. Chem.*, 2012, 1273–1281.
- Hayden F. G.; Couch R. B.: Clinical and Epidemiological Importance of Influenza A Viruses Resistant to Amantadine and Rimantadine, *Rev. Med. Virol.*, 2018, 2 (2), 89–96.
- Moscona A.: Oseltamivir Resistance — Disabling Our Influenza Defenses, *N. Engl. J. Med.*, 2005, 353 (25), 2633–2636.
- Greengard O.; Poltoratskaia N.; Leikina E.; Zimmerberg J.; Moscona A.: The Anti-Influenza Virus Agent 4-GU-DANA (Zanamivir) Inhibits Cell Fusion Mediated by Human Parainfluenza Virus and Influenza Virus HA, *J. Virol.*, 2000, 74 (23), 11108–11114.
- Porotto M.; Murrell M.; Greengard O.; Lawrence M. C.; McKimm-Breschkin J. L.; Moscona A.: Inhibition of Parainfluenza Virus Type 3 and Newcastle Disease Virus Hemagglutinin-Neuraminidase Receptor Binding: Effect of Receptor Avidity and Steric Hindrance at the Inhibitor Binding Sites, *J. Virol.*, 2004, 78 (24), 13911–13919.
- Collins J. P.; Haire F. L.; Lin Y.; Liu J.; Russell J. R.; Walker A. P.; Skehel J. J.; Martin S.; Hay J. A.; Gamblin J. S.: Crystal Structures of Oseltamivir-Resistant Influenza Virus Neuraminidase Mutants, *Nature*, 2008, 453 (7199), 1258–1261.
- Hurt A. C.; Holien J. K.; Parker M.; Kelso A.; Barr I. G.: Zanamivir-Resistant Influenza Viruses with a Novel Neuraminidase Mutation, *J. Virol.*, 2009, 83 (20), 10366–10373.
- Chintakrindi A. S.; Martis E. A. F.; Gohil D. J.; Kothari S. T.; Chowdhary A. S.; Coutinho E. C.; Kanyalkar M. A.: A Computational Model for Docking of Noncompetitive Neuraminidase Inhibitors and Probing Their Binding Interactions with Neuraminidase of Influenza Virus H5N1, *Curr. Comput. Aided. Drug Des.*, 2016, 12 (4), 272–281.
- D'Souza C.; Kanyalkar M.; Joshi M.; Coutinho E.; Srivastava S.: Search for Novel Neuraminidase Inhibitors: Design, Synthesis and Interaction of Oseltamivir Derivatives with Model Membrane Using Docking, NMR and DSC Methods, *Biochim. Biophys. Acta - Biomembr.*, 2009, 1788 (9), 1740–1751.
- Suruse P., Malbari K., Chintakrindi A., Gohil D., Srivastava S., Kothari S., Chowdhary A., Kanyalkar M.: Virucidal Activity of Newly Synthesized Chalcone Derivatives

- against H1N1 Virus Supported by Molecular Docking and Membrane Interaction Studies, **J. Antivir. Antiretrovir. OMICS Int.**, 2016, 8 (2), 79–89.
15. Xu J. J.; Wu X.; Li M. M.; Li G. Q.; Yang Y. T.; Luo H. J.; Huang W. H.; Chung H. Y.; Ye W. C.; Wang G. C.; et al.: Antiviral Activity of Polymethoxylated Flavones from “Guangchenpi”, the Edible and Medicinal Pericarps of Citrus Reticulata ‘Chachi’, **J. Agric. Food Chem.**, 2014, 62 (10), 2182–2189.
 16. Chintakrindi A. S.; Gohil D. J.; Kothari S. T.; Chowdhary A. S.; Kanyalkar M. A.: Design, Synthesis and Evaluation of Chalcones as H1N1 Neuraminidase Inhibitors, **Med. Chem. Res.**, 2018, 27 (4), 1013–1025.
 17. Epand R.; Epand F. R.; McKenzie C. R.: Effects of Viral Chemotherapeutic Agents on Membrane Properties. Studies of Cyclosporin A, Benzyloxycarbonyl-D-Phe-L-Phe-Gly and Amantadine, **J. Biol. Chem.**, 1987; Vol. 262.
 18. McKenzie R. C.; Epand R. M.; Johnson D. C.: Cyclosporine A Inhibits Herpes Simplex Virus-Induced Cell Fusion but Not Virus Penetration into Cells, **Virology**, 1987, 159 (1), 1–9.
 19. Discovery Studio, 3.1; Accelrys Inc., San Diego, USA.
 20. Jones G.; Willett P.; Glen R. C.; Leach A. R.; Taylor R.: Development and Validation of a Genetic Algorithm for Flexible Docking, **J. Mol. Biol.**, 1997, 267 (3), 727–748.
 21. Vavricka C. J.; Li Q.; Wu Y.; Qi J.; Wang M.; Liu Y.; Gao F.; Liu J.; Feng E.; He J.; et al.: Structural and Functional Analysis of Laninamivir and Its Octanoate Prodrug Reveals Group Specific Mechanisms for Influenza NA Inhibition, **PLoS Pathog.**, 2011, 7 (10), e1002249.
 22. Guan L. P.; Zhao D. H.; Chang Y.; Wen Z. S.; Tang L. M.; Huang F. F. Synthesis of 2,4-Dihydroxychalcone Derivatives as Potential Antidepressant Effect, **Drug Res. (Stuttg.)**, 2013, 63 (1), 46–51.
 23. Saxena S.; Makrandi K. J.; Grover K. S.: Cheminform Abstract: Synthesis of 5- And/Or 7-Hydroxyflavones using a Modified Phase Transfer-Catalyzed Baker-Venkataraman Transformation, **Chem. Inform.**, 1985, Vol. 16.
 24. Aue W. P.; Ernst R. R.; B. E.: Two Dimensional Spectroscopy. Application to Nuclear Magnetic Resonance, **J. Chem. Phys.**, 1976, 64 (5), 2229–2246.
 25. Bothner-By A. A.; Stephens R. L.; Lee J.; Warren C. D.; Jeanloz R. W.: Structure Determination of a Tetrasaccharide: Transient Nuclear Overhauser Effects in the Rotating Frame, **J. Am. Chem. Soc.**, 1984, 106 (3), 811–813.
 26. Jeener J.; Meier B. H.; Bachmann P.; Ernst R. R.: Investigation of Exchange Processes by Two-dimensional NMR Spectroscopy, **J. Chem. Phys.**, 1979, 71 (11), 4546–4553.
 27. Li Q.; Qi J.; Zhang W.; Vavricka C. J.; Shi Y.; Wei J.; Feng E.; Shen J.; Chen J.; Liu D.; et al.: The 2009 Pandemic H1N1 Neuraminidase N1 Lacks the 150-Cavity in Its Active Site, **Nat. Struct. Amp; Mol. Biol.**, 2010, 17, 1266.
 28. Reece P. A.: Neuraminidase Inhibitor Resistance in Influenza Viruses, **J. Med. Virol.**, 2007, 79 (10), 1577–1586.
 29. Varghese J. N.; Smith P. W.; Sollis S. L.; Blick T. J.; Sahasrabudhe A.; McKimm-Breschkin J. L.; Colman P. M.: Drug Design against a Shifting Target: A Structural Basis for Resistance to Inhibitors in a Variant of Influenza Virus Neuraminidase, **Structure**, 1998, 6 (6), 735–746.
 30. Chary K. V. R.; Govil G.: NMR in Biological Systems: From Molecules to Human, **Springer Sci. Business Media**, 2008; Vol. 6.
 31. Srivastava S.; Phadke R. S.; Govil G.: Role of Tryptophan in Inducing Polymorphic Phase Formation in Lipid Dispersions, **Indian J. Biochem. Biophys.**, 1988, 25 (3), 283–286.



NOW AVAILABLE ! IDMA-APA GUIDELINES / TECHNICAL MONOGRAPHS

TECHNICAL MONOGRAPH NO. 1
**STABILITY TESTING OF EXISTING
DRUGS SUBSTANCES AND PRODUCTS**

TECHNICAL MONOGRAPH NO. 3
**INVESTIGATION OF OUT OF SPECIFICATION
(OOS) TEST RESULTS**

TECHNICAL MONOGRAPH NO. 5
**ENVIRONMENTAL MONITORING
IN CLEANROOMS**

TECHNICAL MONOGRAPH NO. 7
DATA INTEGRITY GOVERNANCE

TECHNICAL MONOGRAPH NO. 2
**PRIMARY & SECONDARY CHEMICAL
REFERENCE SUBSTANCES**

TECHNICAL MONOGRAPH NO. 4
**PHARMACEUTICAL PREFORMULATION
ANALYTICAL STUDIES**

TECHNICAL MONOGRAPH NO. 6
**CORRECTIVE/PREVENTIVE ACTIONS
(CAPA) GUIDELINE**

Copies are available at IDMA Office, Mumbai. We do not mail any publications against VPP payment. All payments to be made in advance as Cheque/DD/RTGS/NEFT in favour of “**INDIAN DRUG MANUFACTURERS’ ASSOCIATION**” at Mumbai.

For more details please contact: **PUBLICATIONS DEPARTMENT** Tel.: 022 - 2494 4624 / 2497 4308 Fax: 022 - 2495 0723
E-mail: mail_idma@idmaindia.com, Website: www.idma-assn.org/www.indiandrugsonline.org